



Marine Taxa Track Local Climate Velocities
Malin L. Pinsky *et al.*
Science **341**, 1239 (2013);
DOI: 10.1126/science.1239352

This copy is for your personal, non-commercial use only.

If you wish to distribute this article to others, you can order high-quality copies for your colleagues, clients, or customers by [clicking here](#).

Permission to republish or repurpose articles or portions of articles can be obtained by following the guidelines [here](#).

The following resources related to this article are available online at www.sciencemag.org (this information is current as of September 12, 2013):

Updated information and services, including high-resolution figures, can be found in the online version of this article at:

<http://www.sciencemag.org/content/341/6151/1239.full.html>

Supporting Online Material can be found at:

<http://www.sciencemag.org/content/suppl/2013/09/12/341.6151.1239.DC1.html>

This article **cites 21 articles**, 5 of which can be accessed free:

<http://www.sciencemag.org/content/341/6151/1239.full.html#ref-list-1>

arising from the vertical density gradient and the sloping interface

$$\alpha g \int_0^{\delta} (\rho - \rho_{\delta}) dz \quad (1)$$

is balanced by the turbulent shear stress at the interface. With density ρ and layer height δ taken from the CTD profile and basal slope α calculated from depth differences between Drill A and B, the buoyancy force is estimated at 0.043 Pa. This compares favorably to the average shear stress measured by the flux package, $\rho u_*^2 = 0.076$ Pa (Fig. 4B), indicating that the observed boundary layer flow is forced by the melt-generated buoyancy acting along the sloping base of the shelf.

These in situ measurements of the underside of the PIG ice shelf reveal strong but spatially non-uniform ice/ocean interaction, in which ocean boundary layers are strongly coupled to basal melting: They are buoyantly forced by melt water and are constrained by the resulting melt channel morphology. The pRES melt rate estimates document the cross-channel variability in melt rate that results from the channelized flow, whereas the longer-term flux package estimates demonstrate that melt rates and boundary layer properties were fairly steady over the month of observations, which is consistent with the idea that the forcing is due to the relatively slowly evolving buoyancy field within the ocean cavity. If these direct melt rates within the channel are annualized, they range between 14.2 and 24.5 m year⁻¹. However, we expect that melt rates will be affected by seasonal or other long-time-scale variability associated with the oceanic forcing. We also expect along-shelf

spatial variability in cross-shelf melt patterns, as supported by recent altimetry analyses (13) that infer preferential melting of keels toward the terminus. The continuity of the channels seen in satellite imagery and the airborne radar survey, in conjunction with the vigorous melt rates here described, indicate that basal melting is active from the grounding line to at least the mid-shelf location of the observations. In addition to our observations, a recent idealized numerical simulation of an ice shelf base and ocean boundary layer has suggested that channelization is of fundamental importance, because a channelized base actually melts much less vigorously than a nonchannelized one (14). The remarkable ice/ocean coupling evident in our observations points to the need to represent channelized ice/ocean interaction in models of PIG and similar outlet glaciers in global climate simulations of sea-level change.

References and Notes

1. J. L. Bamber, R. E. M. Riva, B. L. Vermeersen, A. M. LeBrocq, *Science* **324**, 901–903 (2009).
2. E. Rignot *et al.*, *Nat. Geosci.* **1**, 106–110 (2008).
3. A. Shepherd, D. J. Wingham, J. A. D. Mansley, H. F. J. Corr, *Science* **291**, 862–864 (2001).
4. D. J. Wingham, D. W. Wallis, A. Shepherd, *Geophys. Res. Lett.* **36**, L17501 (2009).
5. A. J. Payne, A. Vieli, A. P. Shepherd, D. J. Wingham, E. Rignot, *Geophys. Res. Lett.* **31**, L23401 (2004).
6. H. D. Pritchard, R. J. Arthern, D. G. Vaughan, L. A. Edwards, *Nature* **461**, 971–975 (2009).
7. S. S. Jacobs, H. H. Hellmer, A. Jenkins, *Geophys. Res. Lett.* **23**, 957–960 (1996).
8. S. S. Jacobs, A. Jenkins, C. F. Giulivi, P. Dutrieux, *Nat. Geosci.* **4**, 519–523 (2011).
9. A. Jenkins *et al.*, *Nat. Geosci.* **3**, 468–472 (2010).
10. D. G. Vaughan *et al.*, *J. Geophys. Res.* **117**, F03012 (2012).

11. R. Bindshadler, D. G. Vaughan, P. Vornberger, *J. Glaciol.* **57**, 581–595 (2011).
12. J. H. Trowbridge, S. J. Lentz, *J. Phys. Oceanogr.* **28**, 2075–2093 (1998).
13. P. Dutrieux *et al.*, *Cryosphere Discuss* **7**, 1591–1620 (2013).
14. C. V. Gladish, D. M. Holland, P. R. Holland, S. F. Price, *J. Glaciol.* **58**, 1227–1244 (2012).
15. T. Haran, J. Bohlander, T. Scambos, T. Painter, M. Fahnestock, compilers, *Moderate Resolution Imaging Spectroradiometer (MODIS) Mosaic of Antarctica (MOA) Image Map* (National Snow and Ice Data Center, Boulder, CO, 2005, updated 2006) (digital media).
16. E. Rignot, J. Mouginot, B. Scheuchl, *Science* **333**, 1427–1430 (2011).
17. R. Bindshadler *et al.*, *Cryosphere* **5**, 569–588 (2011).

Acknowledgments: Data presented here are archived with the supplementary materials and also as a MATLAB data structure at www.oc.nps.edu/~stanton/pig/data/data.html/PIGSITE1_first35days. The authors acknowledge the contributions of J. Stockel in software development and deployment of the ocean instruments, D. Pomraning in designing and manning the hot-water drill equipment, and M. Shortt for making the British Antarctic Survey pRES field measurements. Outstanding logistic and safety support was provided by K. Gibbon, D. Einerson, E. Steinarsson, F. McCarthy, S. Consalvi, the PIG support camp personnel, and the NSF Antarctic support team. This research project was supported by NSF's Office of Polar Programs under NSF grants including ANT-0732926, funding from NASA's Cryospheric Sciences Program, New York University Abu Dhabi grant 1204, and the Natural Environment Research Council–British Antarctic Survey Polar Science for Planet Earth Program.

Supplementary Materials

www.sciencemag.org/cgi/content/full/341/6151/1236/DC1
Materials and Methods
References (18–21)

19 April 2013; accepted 6 August 2013
10.1126/science.1239373

Marine Taxa Track Local Climate Velocities

Malin L. Pinsky,^{1,2*} Boris Worm,³ Michael J. Fogarty,⁴ Jorge L. Sarmiento,⁵ Simon A. Levin¹

Organisms are expected to adapt or move in response to climate change, but observed distribution shifts span a wide range of directions and rates. Explanations often emphasize biological distinctions among species, but general mechanisms have been elusive. We tested an alternative hypothesis: that differences in climate velocity—the rate and direction that climate shifts across the landscape—can explain observed species shifts. We compiled a database of coastal surveys around North America from 1968 to 2011, sampling 128 million individuals across 360 marine taxa. Climate velocity explained the magnitude and direction of shifts in latitude and depth much more effectively than did species characteristics. Our results demonstrate that marine species shift at different rates and directions because they closely track the complex mosaic of local climate velocities.

Global warming during the past century has had many biological effects, including changes in phenology and poleward shifts in species distributions (1–3). However, species have not responded uniformly, and shifts in their distributions have occurred at widely differ-

ent rates and in different directions (1–10). In both marine and terrestrial assemblages, up to 60% of species are not shifting as expected; i.e., to higher latitudes, higher elevations, or greater depths (1–10). A range of hypotheses has been proposed to explain this observed variation, in-

cluding the effects of habitats (11), species interactions (11, 12), sensitivity to environmental gradients (13), response times (10), colonization abilities (14), and physiological or evolutionary adaptations (15). In essence, many of the leading hypotheses have emphasized biological differences among species (8–10, 14).

An alternative and possibly more general hypothesis posits that local differences in climate velocity (16, 17) can explain heterogeneity in species shifts. Climate velocity is the rate and direction that isotherms shift through space, and it combines both temporal and spatial rates of temperature change (16, 17). Previous authors have hypothesized that species may follow

¹Department of Ecology and Evolutionary Biology, Princeton University, Princeton, NJ 08544, USA. ²Department of Ecology, Evolution, and Natural Resources and the Institute of Marine and Coastal Sciences, Rutgers University, New Brunswick, NJ 08901, USA. ³Department of Biology, Dalhousie University, Halifax, NS B3H 4R2, Canada. ⁴Northeast Fisheries Science Center, Woods Hole, MA 02453, USA. ⁵Atmospheric and Oceanic Sciences Program, Princeton University, Princeton, NJ 08544, USA.

*Corresponding author. E-mail: malin.pinsky@rutgers.edu

climate velocities (16–19), but a direct test has not been attempted (2, 13, 18). An examination of broad taxonomic groups found faster shifts in regions of higher climate velocities but did not examine variation among species or shifts toward lower latitudes (2). These issues are particularly important in the ocean, where climate velocities are up to seven times higher than on land (16, 18).

To understand how marine species respond to climate velocity, we compiled four decades of scientific surveys of fish and invertebrates from the continental shelves of North America across nine regions spanning ~3.3 million km² and 60,394 bottom-trawl samples from 1968 to 2011 (fig. S1 and table S1). These surveys captured 128 million organisms from 580 populations of 360 species or species groups; we refer to these collectively as “taxa.”

We measured range shifts by tracking the location of range centroids (20). Taxa showed considerable variation in the direction and rate of shifts, both within regions (Fig. 1, B to D) and between regions (Fig. 1A and figs. S2 to S4). Individual species shifted north (for example,

American lobster in the northeast), south (big skate on the west coast), or remained approximately stable (Pacific cod in Alaska, Fig. 1). Defining an assemblage as the set of sampled taxa within a geographic region, four assemblages shifted poleward (Fig. 1, A, B, and D), whereas five shifted south (Fig. 1, A and C, and fig. S2). For example, assemblages from the west coast and the Gulf of Alaska shifted south at >11 km/decade during a cooling period that is thought to reflect multidecadal climate variability (21).

At the assemblage level, regional temperature changes explained differences in observed shifts, although modified by geographic constraints. Assemblage shifts were positively but weakly related to bottom temperature trends ($r^2 = 0.27$, $P = 0.15$, $n = 9$ regions; Fig. 2A). However, the Gulf of Mexico assemblage (Fig. 1C) was an outlier in this relationship and the only warming region with an east-west coastline that prevented poleward shifts. Instead, this assemblage shifted deeper (Fig. 2D). After this region was omitted, bottom temperature explained more than half of the variation in assemblage shifts

($r^2 = 0.60$, $P = 0.023$, $n = 8$ regions). Surface temperature trends were not correlated to latitudinal shifts ($P = 0.75$, $r^2 = 0.02$; without the Gulf of Mexico, $P = 0.53$, $r^2 = 0.08$). However, assemblages that experienced increasing surface temperatures tended to shift deeper, away from warming waters ($r^2 = 0.80$, $P = 0.0028$, $n = 8$ regions; Fig. 2D and fig. S5). Depth shifts were not related to bottom temperature changes ($r^2 = 0.12$, $P = 0.36$). These relationships concern whole assemblages, not individual taxa. Individual shifts were weakly correlated to changes in average regional temperature (latitude versus bottom temperature without the Gulf of Mexico: $P = 0.0013$, $r^2 = 0.022$, $n = 474$ taxa; depth versus surface temperature: $P < 0.0001$, $r^2 = 0.05$, $n = 497$ taxa).

Although regional patterns can be informative, they do not reveal the extent to which individual taxa follow local variation in climate velocities. Climate velocities are often calculated for grid cells (16, 17), but taxon distributions are irregular and a taxon-specific version of climate velocity is needed that averages velocities across species’ ranges. We therefore used survey data

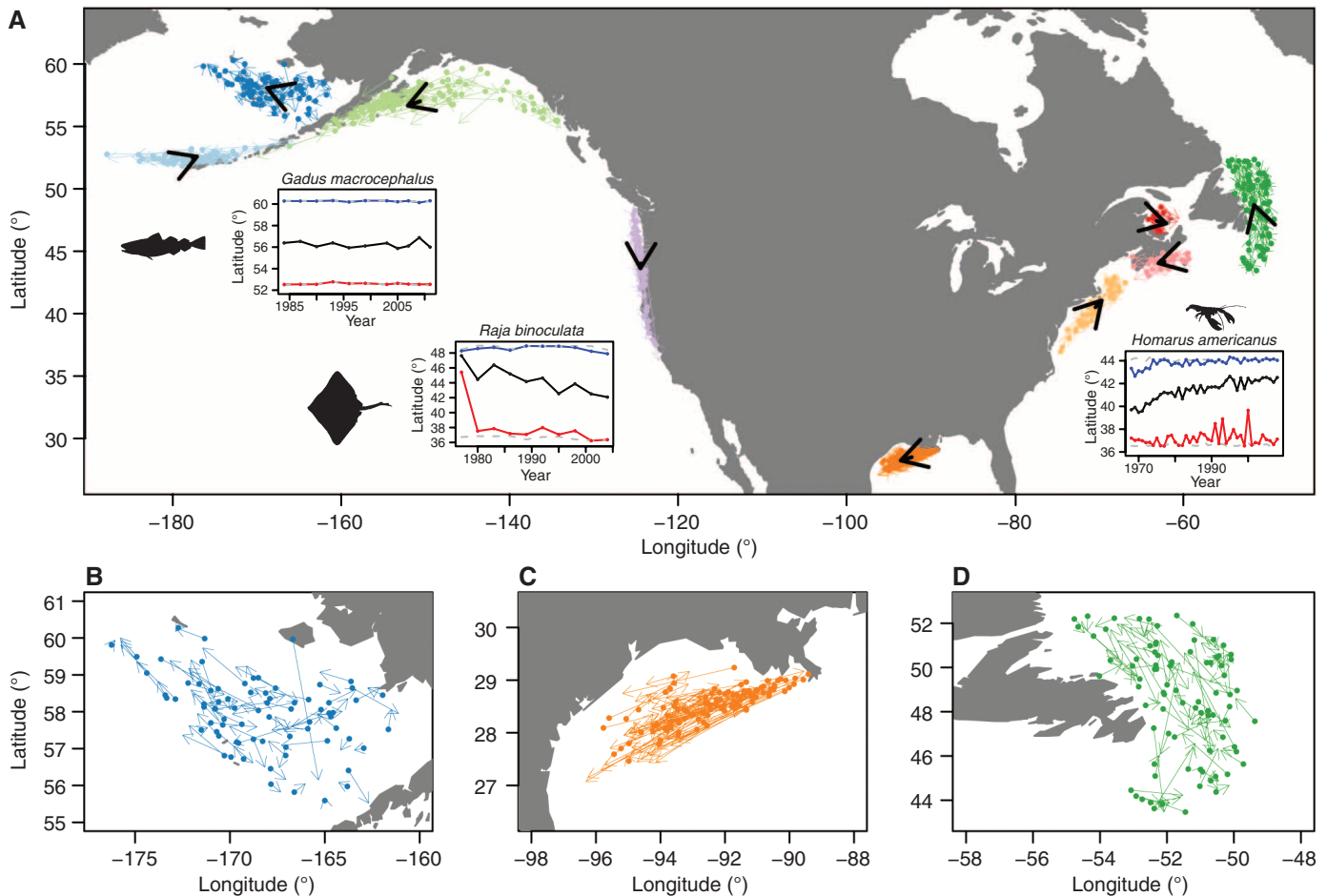


Fig. 1. Shifts in the distribution of marine taxa. (A) Vectors show the average shift in latitude and longitude for each taxon (colors) and the mean shift in each region (black). Insets show the mean (black), maximum (blue), and minimum (red) latitude of detection for Pacific cod (*Gadus macrocephalus*)

in the Gulf of Alaska, big skate (*Raja binoculata*) on the U.S. West Coast, and American lobster (*Homarus americanus*) in the Northeast. Gray dashed lines in insets indicate the range of surveyed latitudes. Detailed views are also shown of (B) the Eastern Bering Sea, (C) the Gulf of Mexico, and (D) Newfoundland.

to calculate the temperature range inhabited by each taxon and measured taxon-specific climate velocity as the rate and direction that these temperatures shifted across the landscape (20). We found considerable spatial variation in climate velocities (Fig. 3). The taxa also showed considerable heterogeneity: 46% shifted south and 58% shifted shallower (Figs. 1 and 3 and figs. S5 and S6).

Such heterogeneity among taxa, however, was not random. Instead, differences in climate velocity explained much of the variation in the rate and direction of latitudinal range shifts ($r^2 = 0.38$, $P < 0.0001$, $n = 325$ taxa; Fig. 3A). The relationship remained significant if random effects for region were included ($P < 0.0001$) or if we used bootstrap resampling to generate a null distribution of correlations ($P = 0.019$) (20). Across all taxa, 74% shifted latitude in the same direction as climate velocity, and 70% shifted depth in the same direction. This explanatory power was equally high for “non-intuitive” shifts

that deviate from the poleward-and-deeper pattern: 73% of shifts to lower latitudes and 75% of shifts toward shallower water were explained by climate velocity.

To estimate whether taxa were shifting faster or slower than climate velocity, we measured the bias [in degrees north ($^{\circ}$ N) per year] as well as relative bias between taxon-specific velocities and observations (20). However, we found that taxa on average do not lag (bias: $P = 0.13$, mean = 0.003 $^{\circ}$ N/year; relative bias: $P = 0.39$, mean = 4.68).

Climate velocity can also be projected across depth, and we found evidence that climate velocities can explain variation in the rate and direction that taxa shifted shallower or deeper ($r^2 = 0.13$, $P < 0.0001$, $n = 325$ taxa; Fig. 3B and fig. S7). Depth biases were not significantly different from zero (bias: $P = 0.60$, mean = -0.040 m/year; relative bias: $P = 0.49$, mean = 3.8), again indicating little to no lag in species response to changing climate.

Fig. 2. Relationships between sea temperature change and assemblage shifts. (A) Latitude shifts versus bottom temperature (the black circle marks the Gulf of Mexico), (B) latitude shifts versus surface temperature, (C) depth shifts and bottom temperature, and (D) depth shifts and surface temperature. Positive depth shifts are toward deeper water. Error bars show standard errors, and colors match the taxon vectors in Fig. 1.

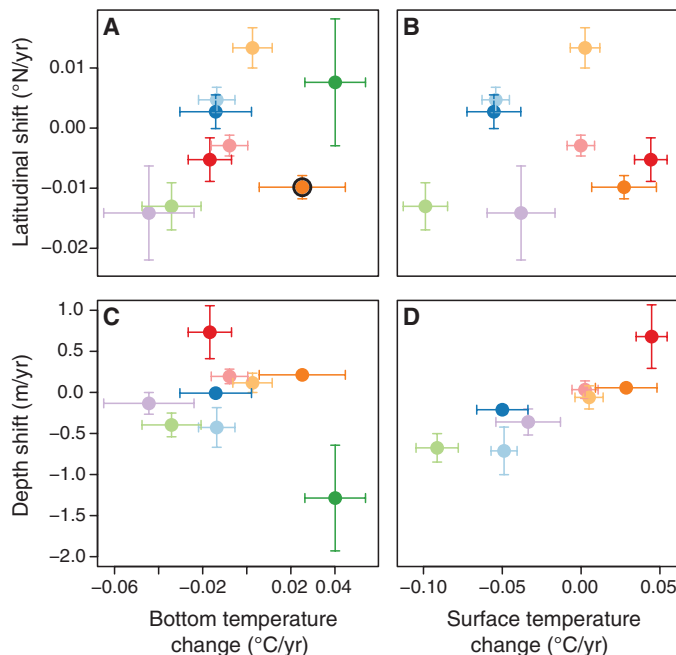
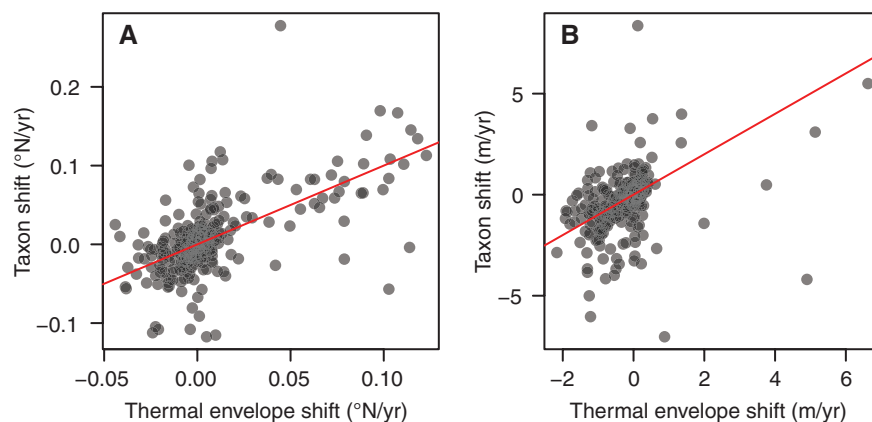


Fig. 3. Climate velocity and taxon shifts. The relationship between taxon-specific climate velocities and observed shifts in taxon range centroids is shown for (A) shifts in latitude and (B) shifts in depth. The 1:1 line is shown in red.



There was little evidence that other factors could explain variation in the speed and direction of taxon shifts. For example, adding survey and species characteristics to a multiple regression model only increased the explained variance in species shifts for all taxa from 38% (model with climate velocity as the only explanatory variable) to 42% (full model with all variables), or from 36 to 45% for fish (Table 1 and table S5). Survey and species characteristics, however, may be more likely to influence the speed (absolute value of $^{\circ}$ N/year) rather than the combined speed and direction of observed shifts. Higher relative variable importance (RVI) for survey extent and duration, as well as for climate velocity (table S4), suggested that the most rapidly shifting species might not appear in our analysis because they left the survey area. There was also limited evidence that invertebrates, commercially fished taxa, pelagic taxa, taxa with declining biomass, fish with small ranges, fish higher in the food chain, and large fish shifted faster (tables S4 and S5). Such species characteristics, however, explained at most 1.3% of the variation in speed across all taxa (3.3% across all fish), as compared to 18% for climate velocity (or 20% across all fish). We conclude that variation in the environment is a much more powerful predictor of taxon shifts than variation in life history.

A previous study also found that species traits had little power to explain distribution shifts, but it did not examine climate velocities (14). Likewise, climate heterogeneity has been connected to the direction but not magnitude of shifts in birds and fish (3, 5, 7, 13). Recognizing and quantifying heterogeneity in climate velocities across multiple scales may substantially improve our ability to explain ecological changes and project into the future. Our findings suggest that bioclimate envelope methods are valuable (19) but can be improved by the use of fine-scale climate data.

Beyond climate velocity, other influences on species shifts probably include species interactions (12), fisheries harvest, habitat, and species' abilities to disperse and adapt (14, 15). Release from a poleward-shifting predator, for example,

Table 1. Models explaining the direction and speed (°N/year) of latitudinal shifts in taxon distributions. Models were fit to data either for all taxa (top section, $n = 325$ taxa) or for fish alone (bottom section, $n = 199$ taxa). RVI ranks all explanatory variables from high to low importance. The model coefficients associated with each variable are shown for the most parsimonious model with the lowest Akaike information criterion (AIC) value (best model); a model with all factors retained (full model); a multimodel average (model

average); and models with only climate velocity, only survey characteristics (survey char.), or only species characteristics (species char.) retained as explanatory variables. The Δ AIC indicates the difference in model parsimony as explained by AIC relative to the best model; a Δ AIC value <10 indicates higher support for a model. Values of r^2 and Akaike weight for each model are also shown. RVI and Akaike weights were calculated across all possible models (128 for all taxa, 1024 for fish alone).

Variable	RVI	Best model	Full model	Model average	Climate velocity	Survey char.	Species char.
<i>All taxa</i>							
Climate velocity	1	0.92	0.87	0.9	0.96		
Survey extent	0.505		0.00093	0.00044		0.005	
Survey duration	0.3		0.00015	1.80×10^{-5}		0.0012	
Fish/invert.	0.796	0.011	0.0098	0.0084			0.02
Unfished/fished	0.848	-0.0087	-0.0085	-0.0079			-0.0099
Pelagic/demersal	0.776	0.016	0.014	0.012			0.024
Biomass trend	0.45		0.0048	0.0023			0.0056
Δ AIC		0	2.52		11.1	127	145
r^2		0.41	0.42		0.38	0.12	0.081
Akaike weight		0.11	0.03		0.00041	3.50×10^{-29}	2.90×10^{-33}
<i>Fish</i>							
Climate velocity	1	0.76	0.77	0.78	0.93		
Survey extent	0.838	0.0023	0.0017	0.0018		0.0063	
Survey duration	0.42		-0.00041	-0.00021		0.00074	
Growth rate	0.3		-0.0016	-0.00066			-0.0091
Unfished/fished	0.41		-0.0068	-0.0028			-0.0025
Pelagic/demersal	0.947	0.028	0.023	0.025			0.041
Range size	0.286		3.70×10^{-5}	1.30×10^{-5}			0.00013
Biomass trend	0.344		0.0034	0.0013			0.0046
Trophic level	0.356		-0.0061	-0.0022			-0.005
Maximum length	0.956	0.014	0.014	0.014			0.013
Δ AIC		0	8.63		20.4	72.1	95.9
r^2		0.44	0.45		0.36	0.18	0.13
Akaike weight		0.071	0.00095		2.60×10^{-6}	1.50×10^{-17}	1.10×10^{-22}

could drive a prey's range centroid toward lower latitudes. However, even such shifts would be subject to the physiological constraints imposed by thermal conditions.

We find that marine taxa follow climate velocities with surprising accuracy, a pattern that holds largely irrespective of individual life histories. Hence, it appears that much of the seemingly individualistic variation in the magnitude and direction of species range shifts can be explained by local variation in climate velocity. Our results contrast with evidence that terrestrial species lag behind climate velocity (4, 10) [though see (5)] and suggest that marine species may be better able to keep pace with climate change. Marine species may shift more rapidly than species on land because they face fewer barriers to dispersal and more completely fill their thermal niches (6). However, the observed rapid range shifts will fundamentally reorganize marine communities. Climate-induced movements of highly commercial species have already sparked cross-border fisheries conflicts, and they can confound traditional management approaches (8). Forecasts of climate velocity may provide an important tool to anticipate the scale and magnitude of these impacts now and into the future.

References and Notes

1. C. Parmesan, G. Yohe, *Nature* **421**, 37–42 (2003).
2. I.-C. Chen, J. K. Hill, R. Ohlemüller, D. B. Roy, C. D. Thomas, *Science* **333**, 1024–1026 (2011).
3. A. L. Perry, P. J. Low, J. R. Ellis, J. D. Reynolds, *Science* **308**, 1912–1915 (2005).
4. K. Zhu, C. W. Woodall, J. S. Clark, *Glob. Change Biol.* **18**, 1042–1052 (2012).
5. N. K. Dulvy *et al.*, *J. Appl. Ecol.* **45**, 1029–1039 (2008).
6. J. M. Sunday, A. E. Bates, N. K. Dulvy, *Nat. Clim. Change* **2**, 686 (2012).
7. J. A. Nye, J. S. Link, J. A. Hare, W. J. Overholtz, *Mar. Ecol. Prog. Ser.* **393**, 111–129 (2009).
8. F. J. Muester, M. A. Litzow, *Ecol. Appl.* **18**, 309–320 (2008).
9. C. Moritz *et al.*, *Science* **322**, 261–264 (2008).
10. F. A. La Sorte, W. Jetz, *J. Anim. Ecol.* **81**, 914–925 (2012).
11. J. Lenoir *et al.*, *Ecography* **33**, 295 (2010).
12. R. K. Heikkinen, M. Luoto, R. Virkkala, R. G. Pearson, J.-H. Körber, *Glob. Ecol. Biogeogr.* **16**, 754–763 (2007).
13. M. W. Tingley, M. S. Koo, C. Moritz, A. C. Rush, S. R. Beissinger, *Glob. Change Biol.* **18**, 3279–3290 (2012).
14. A. L. Angert *et al.*, *Ecol. Lett.* **14**, 677–689 (2011).
15. L.-M. Chevin, R. Lande, G. M. Mace, *PLoS Biol.* **8**, e1000357 (2010).
16. M. T. Burrows *et al.*, *Science* **334**, 652–655 (2011).
17. S. R. Loarie *et al.*, *Nature* **462**, 1052–1055 (2009).
18. R. Ohlemüller, *Science* **334**, 613–614 (2011).

19. W. W. L. Cheung *et al.*, *Fish Fish.* **10**, 235–251 (2009).
20. Materials and methods are available as supplementary materials on Science Online.
21. F. P. Chavez, M. Messié, J. T. Pennington, *Annu. Rev. Mar. Sci.* **3**, 227–260 (2011).

Acknowledgments: We thank H. Benoît, B. Brodie, D. Clark, L. Col, J. Hare, B. Horness, R. Lauth, M. McClure, N. Peaks, J. Pearl, J. Rester, and M. Wilkins for assistance with data; C. Beaulieu, P. Kareiva, R. Rykaczewski, A. Smith, C. Stock, and J. Watson for helpful conversations; and M. Tingley, O. Jensen, and K. Hunter-Thomson for comments on the manuscript. Funding was provided by a David H. Smith Conservation Research Fellowship (M.L.P.), the Natural Sciences and Engineering Research Council of Canada (B.W.), the Nippon Foundation—University of British Columbia Nereus Program (J.L.S.), and NSF (S.A.L.). M.L.P. designed the study; M.L.P. and M.J.F. assembled the data; M.L.P., B.W., and M.J.F. analyzed the data; and M.L.P. and B.W. wrote the paper. S.A.L. and J.L.S. supervised the project. Locations of source data used in our analysis can be found in the supplementary materials.

Supplementary Materials
www.sciencemag.org/cgi/content/full/341/6151/1239/DC1
 Materials and Methods
 Figs. S1 to S6
 Tables S1 to S5
 References (22–26)
 18 April 2013; accepted 13 August 2013
 10.1126/science.1239352